Steel and Composite Structures, *Vol. 26, No. 1 (2018) 79-87*
DOI: https://doi.org/10.12989/scs.2018.26.1.079

Analysis on natural vibration characteristics of steel-concrete composite truss beam

Lizhong Jiang[1,2a], Yulin Feng[1b], Wangbao Zhou[*1,2] and Binbin He[3c]

[1]*School of Civil Engineering, Central South University, Changsha, 410075, China*
[2]*National Engineering Laboratory for High Speed Railway Construction, Central South University, Changsha, 410075, China*
[3]*State Key Laboratory of Frozen Soil Engineering, Northwest Institute of Eco-Environment and Resources, CAS, Lanzhou, 730000, China*

(*Received March 18, 2017, Revised May 30, 2017, Accepted September 29, 2017*)

Abstract. In order to study the natural vibration characteristics of steel-concrete composite truss beam (SCCTB), the influence of multiple factors such as interface slip, shear deformation and moment of inertia are considered. Afterwards, based on the Hamilton principle the vibration control differential equation and natural boundary conditions of SCCTB are deduced. By solving SCCTB differential equations of vibration control, an analytical calculation method is proposed for analyzing the natural vibration characteristics of SCCTB. The natural frequencies of SCCTBs with different degrees of shear connection and effective lengths are calculated by using the analytical method, and the results are compared against those obtained from ANSYS finite element numerical calculation method. The results show that the analytical method considering the influence factors such as interface slip, shear deformation and moment of inertia are in good agreement with those obtained from ANSYS finite element numerical calculation method. This evidences the correctness of the analytical method and show that the method proposed exhibits improvement over the previously developed theories for the natural vibration characteristics of SCCTB. Finally, based on the analytical method, the influence factors of SCCTB natural vibration characteristics are analyzed. The results indicate that the influence of interface slip stiffness on SCCTB's natural frequency is more than 10% and therefore cannot be neglected. Moreover, shear deformation has an effect of more than 35% on SCCTB's natural frequency and the effect cannot be ignored either in this case too.

Keywords: steel-concrete composite truss; natural vibration characteristics; shear deformation; interface slip; degree of shear connection; analytical solution

1. Introduction

Steel-concrete composite truss beam (SCCTB) is made up of steel truss and concrete slab. Steel truss and concrete slab are connected through stud connectors so that the two can bear the applied load together. It will help to take full advantage of compressive performance of concrete slab, shear and tensile performance of steel truss. SCCTB has a large bending stiffness and excellent seismic performance, so it is suitable for large-span bridge structures. The stud connectors between steel truss and concrete slab cannot be absolutely rigid. Even for a full composite design, the deflection obtained by ignoring the interface slip effect will be underestimated as compared to the experimental measurements. This indicates that the mechanical property of SCCTB is influenced by the slip effect (Nie *et al*. 2004, Nie *et al*. 2007, Ding *et al*. 2016, Liu *et al*. 2016, Zhou *et al*. 2016).

At present, the researches on the mechanical properties of SCCTB are limited in technical literature domain. Giltner and Kassimali (2000) developed a method of equivalent beam to replace the trusses with the beam elements, which reduces the size of the computer model required for analysis. Machacek and Cudejko (2009, 2010, 2011) has conducted experimental study and theoretical analysis of the interface longitudinal shear force distribution of SCCTB. Bouchair *et al.* (2012) proposed a calculation method to control interface relative slip by using shear stud connectors. Bujnak and Bouchair (2014) has compared the result from finite element numerical calculation method with the experimental results. They found that the local effects of concentrated longitudinal shear forces should be appropriately examined in SCCTB having the welded headed studs, located at the steel-concrete interface. Several effects on shear connection behaviour are also studied, for e.g., Chan and Fong (2011a) has done some experimental study and theoretical analysis, and concluded that the use of effective length method in linear analysis and design method is less convenient and accurate than the second-order analysis. On the basis of literature (Chan and Fong 2011a), Fong *et al.* (2011b) further proved that the second-order analysis method was not only an accurate design method, but also avoid the uncertain approximate value of the effective length. Duratna *et al.* (2013) analyzed the

∗Corresponding author, Ph.D.
E-mail: zhouwangbao@163.com
[a]Ph.D.
E-mail: lzhjiang@csu.edu.cn
[b]Ph.D.
E-mail: fylin119@csu.edu.cn
[c]Ph.D.
E-mail: hebinbin@lzb.ac.cn

ISSN: 1229-9367 (Print), 1598-6233 (Online)

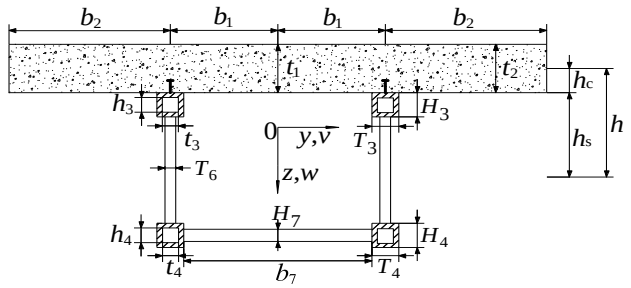

Fig. 1 SCCTB cross-sectional size and coordinate system

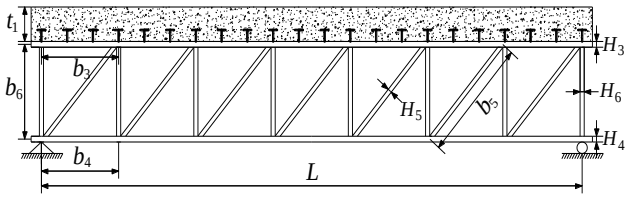

Fig. 2 SCCTB structural design

behavior of SCCTB based on a finite element model and the parametric study including the diameter of the shear connectors, the degree of connection, the top chord section, and the material characteristics. The results showed that the shear connection in SCCTB reduces its deflection by approximately 50% in comparison to the steel truss. Further, a significant influence of the top chord section on the shear forces in the shear connectors was also observed. In order to completely understand the actual capacity of the SCCTB to transfer the shear stresses from the bottom plate of the truss to the concrete, significant theoretical and experimental work has been carried out. The SCCTB is typically composed by a steel plate or a precast concrete slab working as bottom chord, a system of ribbed or smooth steel rebars welded to form the diagonals of the truss and coupled rebars used to form the upper chord (Aiello 2008, Colajanni *et al.* 2014, 2015a). Siekierski (2016a) analyzed the effects of shrinkage of concrete slab in SCCTB and developed a set of linear equations to compute the axial forces in members of the flange of truss girder and transverse shear forces in SCCTB. Campione *et al.* (2016), Colajanni *et al.* (2017) studied the evaluation of the shear resistance of the connections between the bottom chord and concrete slab through the oblique web members of SCCTB and developed a mechanical model that could account for the particular issues arising in this beam typology. The contribution of the steel plate was taken into account in the resisting mechanism. The experimental and numerical results of the two references were employed for the validation of the proposed analytical expressions. Colajanni *et al.* (2015b) had dealt with the flexural response of composite trussed beams connected to R.C. columns, and focusing on the evaluation of strength, rotational capacity and ductility of the end sections of the beam, the plastic hinges were usually placed. Siekierski (2016b) developed an analytical method, focusing on the evaluation of strength, rotational capacity and ductility of the end sections of the beam in which the plastic hinges were usually placed for the estimation of the natural bending frequency of SCCTB. Computed results were compared with frequencies recorded during bridge testing, and the results showed that taking into consideration the joint action of the truss beams and the composite deck, as well as the limited shear stiffness provided by diagonal bracing, would significantly improve the accuracy of the assessment provided by the analytical method. The static behavior of SCCTB was analyzed in detail using the linear finite element method by (Han *et al.* 2005). Han (2004) calculated the natural frequencies and mode shapes of SCCTB by subspace iterative method, and all kinds of influencing factors including pre-stress of cables, boundary condition, decentration of plate and rib, span-to-height ratio, added mass and node stiffness were analyzed.

It can be seen from the above literatures that the mechanical properties of SCCTB are affected by shear deformation and interface slip effect. However, the study on natural vibration characteristic of SCCTB with comprehensive consideration of shear deformation and interface slip effect is very limited. Therefore, by using the Hamilton principle, the influence of multiple factors such as slip, shear deformation and moment of inertia of SCCTB are considered and the natural vibration characteristics of SCCTB are analyzed by using the analytical method. Finally, the results of the analytical solution are compared with those of the ANSYS finite element calculation and the correctness of the analytical solution is verified. It will lay the theoretical foundation for further development of the dynamic characteristics of SCCTB, and can draw some meaningful conclusions for engineering design.

2. Basic assumptions

The cross-sectional size and coordinate system of SCCTB are both shown in Fig. 1, and SCCTB structural design is shown in Fig. 2. According to the characteristics of SCCTB, the following simplified assumptions can be made in order to simplify the calculation.

The analysis of natural vibration frequency of SCCTB is carried out based on assumptions of small deformation and both of steel and concrete materials being in elastic stage.

The longitudinal displacements of the upper chords, lower chords and the concrete slab could be expressed as the superposition of the longitudinal displacement meeting the respective plane cross-section assumption and the longitudinal displacement caused by the interface slip, and can be expressed as

$$u_{\mathrm{x}i}(x,y,z,t)=k_{\mathrm{c}}\xi(x,t)-(z-z_{\mathrm{t}})\theta(x,t) \quad i=1,2 \tag{1}$$

$$u_{\mathrm{x}i}(x,y,z,t)=k_{\mathrm{s}}\xi(x,t)-(z-z_{\mathrm{s}})\theta(x,t) \quad i=3,4 \tag{2}$$

According to the literatures (Zhou *et al.* 2012, Zhou *et al.* 2013, Zhou *et al.* 2013, Zhou *et al.* 2015), the following equations can be obtained

$$k_{\mathrm{c}}=-A_{\mathrm{s}}/A_0, \quad k_{\mathrm{s}}=A_{\mathrm{c}}/(nA_0) \tag{3}$$

where, u_{xi} (i=1,2,3,4) are the longitudinal displacements of concrete roof slab, concrete cantilever slab, upper chord and

lower chord, respectively; $\theta(x,t)$ is cross-section rotation function of concrete slab and steel truss; $\xi(x,t)$ is the difference between the longitudinal displacements at centroids of concrete slab and steel truss; $2b_1$ and b_2 are widths of the concrete roof and cantilever slabs respectively; t_1 and t_2 are thicknesses of concrete roof and cantilever slabs, respectively; b_3, b_4, b_5, b_6, b_7 and b_8 are lengths of the upper chord, lower chord, oblique web member, vertical web member, lower horizontal connection member and oblique bracing member, respectively; L is the effective span of SCCTB; H_3, T_3, h_3 and t_3 are the height and width of external and inner walls of upper chord; H_4, T_4, h_4 and t_4 are the height and width of external and inner walls of lower chord; H_5, T_5, h_5 and t_5 are the height and width of external and inner walls of oblique web member; H_6, T_6, h_6 and t_6 are the height and width of external and inner walls of vertical web member; H_7, T_7, h_7 and t_7 are the height and width of external and inner walls of lower horizontal connection member; H_8, T_8, h_8 and t_8 are the height and width of external and inner walls of oblique bracing member; z_t, z_b and z_s are the coordinates in z direction of centroids of concrete slab, lower chord and steel truss, respectively; $n=E_s/E_c$, where E_s is the elastic modulus of steel truss and E_c is that of the concrete slab; $A_1=2b_1t_1$; $A_2=2b_2t_2$; $A_3=2(H_3T_3-h_3t_3)$; $A_4=2(H_4T_4-h_4t_4)$; $A_5=2(H_5T_5-h_5t_5)$; $A_6=2(H_6T_6-h_6t_6)$; $A_7=H_7T_7-h_7t_7$; $A_8=H_8T_8-h_8t_8$; $A_c=A_1+A_2$ is the cross-section area of concrete slab; $A_{xg}=A_3+A_4$ is the sum of cross-section areas of upper and lower chords; $A_s=A_{xg}+A_5\sin^3\alpha+A_8\cos^3\beta$ is the sum of effective cross-section areas of members in steel truss; α is the angle between oblique and vertical web members; β is the angle between horizontal connection member and oblique bracing members; $A_0=A_c/n+A_s$.

3. Vibration control differential equations of SCCTB and their solutions

3.1 Expressions for strain and stress of each point within cross-section

The axial displacement of the oblique web member can be given by

$$\Delta_5=\delta_1\cos\alpha \tag{4}$$

$$\delta_1=b_4\left(w'-\theta\right) \tag{5}$$

Based on the above expression for longitudinal displacement of cross-section, the expressions for strain at each point in cross-section of SCCTB can be expressed as follows

$$\varepsilon_{\mathrm{xi}}=k_{\mathrm{c}}\frac{\partial\xi}{\partial x}-\left(z-z_{\mathrm{t}}\right)\frac{\partial\theta}{\partial x}\quad i=1,2 \tag{6}$$

$$\varepsilon_{\mathrm{xi}}=k_{\mathrm{s}}\frac{\partial\xi}{\partial x}-\left(z-z_{\mathrm{s}}\right)\frac{\partial\theta}{\partial x}\quad i=3,4 \tag{7}$$

$$\varepsilon_{\mathrm{fg}}=\frac{\Delta_5}{b_5}=\frac{b_4b_6}{b_5^2}\left(w'-\theta\right) \tag{8}$$

$$\varepsilon_{\mathrm{xc}}=\left[k_{\mathrm{s}}\frac{\partial\xi}{\partial x}-\left(z-z_{\mathrm{s}}\right)\frac{\partial\theta}{\partial x}\right]\cos^2\beta \tag{9}$$

$$\gamma_{\mathrm{xz}}=w'-\theta \tag{10}$$

where, ε_{xi} (i=1,2,3,4) are the normal strains of concrete roof slab, concrete cantilever slab, upper chord and lower chord, respectively; ε_{fg} is the normal strain of oblique web member; γ_{xz} is the shear strain of the chords; ε_{xc} is the normal strain of oblique bracing member.

According to assumption, the longitudinal relative slip $\zeta(x,t)$ between slab and truss can be obtained by Eq. (1) and Eq. (2)

$$\zeta\left(x,t\right)=\xi+h_{\mathrm{c}}\theta+h_{\mathrm{s}}\theta=\xi+h\theta \tag{11}$$

where, $h=h_c+h_s$; h_c and h_s are the distances from the centroids of concrete slab and steel truss to the interface, respectively.

According to the above strain model, the stress at each point of cross-section of SCCTB can be expressed as follows

$$\sigma_{\mathrm{xi}}=E_{\mathrm{c}}\left[k_{\mathrm{c}}\frac{\partial\xi}{\partial x}-\left(z-z_{\mathrm{t}}\right)\frac{\partial\theta}{\partial x}\right]\quad i=1,2 \tag{12}$$

$$\sigma_{\mathrm{xi}}=E_{\mathrm{s}}\left[k_{\mathrm{s}}\frac{\partial\xi}{\partial x}-\left(z-z_{\mathrm{s}}\right)\frac{\partial\theta}{\partial x}\right]\quad i=3,4 \tag{13}$$

$$\sigma_{\mathrm{fg}}=E_{\mathrm{s}}\frac{b_4b_6}{{b_5}^2}\left(\frac{\partial w}{\partial x}-\theta\right) \tag{14}$$

$$\varsigma\left(x,t\right)=k_{\mathrm{sl}}\zeta\left(x,t\right)=k_{\mathrm{sl}}\left(\xi+h\theta\right) \tag{15}$$

$$\tau_{\mathrm{xz}}=G_{\mathrm{s}}(\frac{\partial w}{\partial x}-\theta) \tag{16}$$

Interface slip stiffness can be expressed as (Nie *et al.* 2005, Zhou *et al.* 2016)

$$k_{\mathrm{sl}}=k_1/l_{\mathrm{s}},\quad k_1=0.66n_{\mathrm{s}}V_{\mathrm{u}},\quad V_{\mathrm{u}}=A_{\mathrm{s}}f_{\mathrm{s}}rl_{\mathrm{s}}/\left(Ln_{\mathrm{s}}\right) \tag{17}$$

where, l_s is the longitudinal distance of stud connectors; n_s is the number of stud connectors in each row; V_u is the shear resistance of single stud; f_s is the tensile strength of stud; r is the degree of shear connection; G_s is the steel shear modulus; k_{sl} is the interface slip stiffness; k_1 is the stiffness of single stud.

3.2 Strain energy and kinetic energy of SCCTB

The strain energy of SCCTB can be expressed as follows

$$\begin{aligned}V=\frac{1}{2}\int_L\Bigg(&\sum_{i=1}^{4}\int_{A_{\mathrm{i}}}\sigma_{\mathrm{xi}}\varepsilon_{\mathrm{xi}}\mathrm{d}A+\int_{A_{\mathrm{xg}}}\tau_{\mathrm{xz}}\gamma_{\mathrm{xz}}\mathrm{d}A\\&+\int_{A_5}\frac{b_5}{b_4}\sigma_{\mathrm{fg}}\varepsilon_{\mathrm{fg}}\mathrm{d}A+\int_{A_8}\frac{b_4}{b_8}\sigma_{\mathrm{xc}}\varepsilon_{\mathrm{xc}}\mathrm{d}A+\varsigma\zeta\Bigg)\mathrm{d}x\end{aligned} \tag{18}$$

Substituting Eqs. (6)-(16) into Eq. (18), we can obtain as

$$V=\frac{1}{2}\int_L\left[D\xi'^2-2J\xi'\theta'+I\theta'^2+\varsigma\zeta+F(w'-\theta)^2\right]\mathrm{d}x \tag{19}$$

$$D = E_c k_c^2 A_c + E_s k_s^2 A_{xg} + E_s k_s^2 A_8 \left(\frac{b_4}{b_8}\right)^3 \tag{20}$$

$$J = k_c \int_{A_c} E_c (z - z_t)\, dA + k_s \int_{A_{xg}} E_s (z - z_s)\, dA + k_s \left(\frac{b_4}{b_8}\right)^3 A_8 E_s (z_b - z_s) \tag{21}$$

$$I = \int_{A_c} E_c (z - z_t)^2\, dA + \int_{A_{xg}} E_s (z - z_s)^2\, dA + \left(\frac{b_4}{b_8}\right)^3 A_8 E_s (z_b - z_s)^2 \tag{22}$$

$$F = E_s A_5 \frac{b_4 b_6^2}{b_5^3} + G_s A_{xg} \tag{23}$$

The total kinetic energy with consider of moment of inertia can be obtained as

$$T = \frac{1}{2}\int_L \left(m\dot{w}^2 + \sum_{i=1}^{4}\int_{A_i} \rho_i \dot{u}_i^2 \mathrm{d}A + \int_{A_{eq}} \rho_s \dot{\mu}^2 \mathrm{d}A + \frac{b_8}{b_4}\int_{A_8} \rho_s \dot{u}^2 \mathrm{d}A \right) \mathrm{d}x \tag{24}$$

where, $m = \sum_{i=1}^{8} m_i$; $m_1=\rho_c A_1$; $m_2=\rho_c A_2$; $m_3=\rho_s A_3$; $m_4=\rho_s A_4$; $m_5=\rho_s A_{eq}$; $m_6=\rho_s A_{6eq}$; $m_7=\rho_s A_{7eq}$; $m_8=\rho_s A_{8eq}$; A_{eq}, A_{6eq}, A_{7eq} and A_{7eq} are the longitudinal equivalent areas of oblique web member, vertical web member, lower horizontal connection and oblique bracing member, respectively; $A_{eq}=A_5 b_5/b_4$ is the equivalent cross-section area of oblique web member; $t_{eq}=A_{eq}/b_6$ is the equivalent cross-section thickness of oblique web member; ρ_c is the concrete density; ρ_s is the steel density.

By substituting Eqs. (1) and (2) into Eq. (24), the total kinetic energy can be obtained as

$$T = \frac{1}{2}\int_L \left(m\dot{w}^2 + D_1\dot{\xi}^2 - 2J_1\dot{\xi}\dot{\theta} + I_1\dot{\theta}^2 \right) \mathrm{d}x \tag{25}$$

$$D_1 = \rho_c k_c^2 A_c + \rho_s k_s^2 A_{xg} + \rho_s k_s^2 A_{eq} + \frac{b_8}{b_4}\rho_s k_s^2 A_8 \tag{26}$$

$$J_1 = \int_{A_c} \rho_c k_c (z - z_t)\mathrm{d}A + \int_{A_{xg}} \rho_s k_s (z - z_s)\mathrm{d}A + \int_{A_{eq}} \rho_s k_s (z - z_s)\mathrm{d}A + \frac{b_8 k_s A_8 \rho_s}{b_4}(z_b - z_s) \tag{27}$$

$$I_1 = \int_{A_c} \rho_c (z - z_t)^2\, \mathrm{d}A + \int_{A_{xg}} \rho_s (z - z_s)^2\, \mathrm{d}A + \int_{A_{eq}} \rho_s (z - z_s)^2\, \mathrm{d}A + \frac{b_8}{b_4} A_8 \rho_s (z_b - z_s)^2 \tag{28}$$

where, "˙" and "′" represents the partial derivatives of the time t and coordinate x, respectively (similarly hereinafter).

3.3 Vibration control differential equations and boundary conditions

The total potential energy of the SCCTB can be expressed as

$$\int_{t_0}^{t_1}(T - V)\mathrm{d}t = \frac{1}{2}\int_{t_0}^{t_1}\int_0^L \left[m\dot{w}^2 + D_1\dot{\xi}^2 - 2J_1\dot{\xi}\dot{\theta} + I_1\dot{\theta}^2 - D\xi'^2 + 2J\xi'\theta' - I\theta'^2 - F(w' - \theta)^2 + \varsigma\zeta \right] \mathrm{d}x\mathrm{d}t \tag{29}$$

Based on the Hamilton principle (Morassi *et al.* 2007), bending vibration differential equations and natural boundary conditions of SCCTB can be expressed as

$$D\xi'' - k_{sl}\zeta - J\theta'' + J_1\ddot{\theta} - D_1\ddot{\xi} = 0 \tag{30}$$

$$F(w'' - \theta') - m\ddot{w} = 0 \tag{31}$$

$$I\theta'' - J\xi'' - k_{sl}\zeta h + J_1\ddot{\xi} - I_1\ddot{\theta} + F(w' - \theta) = 0 \tag{32}$$

$$(D\xi' - J\theta')\delta\xi\big|_0^L = 0 \tag{33}$$

$$F(w' - \theta)\delta w\big|_0^L = 0 \tag{34}$$

$$(I\theta' - J\xi')\delta\theta\big|_0^L = 0 \tag{35}$$

3.4 Solution of vibration control differential equations of SCCTB

Let

$$\xi(x,t) = \xi_1(x)\sin(\omega t + \varphi) \tag{36}$$

$$w(x,t) = w_1(x)\sin(\omega t + \varphi) \tag{37}$$

$$\theta(x,t) = \theta_1(x)\sin(\omega t + \varphi) \tag{38}$$

where, $\xi_1(x)$, $w_1(x)$ and $\theta_1(x)$ are the amplitude functions.

Let

$$\lambda^k = \frac{\partial^k}{\partial x^k} \tag{39}$$

By substituting Eqs. (36)-(38) into Eqs. (30)-(32), we can obtain

$$(D\lambda^2 - k_{sl} + D_1\omega^2)\xi_1 - (J\lambda^2 + J_1\omega^2 + k_{sl}h)\theta_1 = 0 \tag{40}$$

$$(F\lambda^2 + m\omega^2)w_1 - F\lambda\theta_1 = 0 \tag{41}$$

$$(-J\lambda^2 - k_{sl}h - J_1\omega^2)\xi_1 + F\lambda w_1 + (I\lambda^2 - k_{sl}h^2 + I_1\omega^2 - F)\theta_1 = 0 \tag{42}$$

$$\begin{vmatrix} D\lambda^2 - k_{sl} + D_1\omega^2 & 0 & -J\lambda^2 - J_1\omega^2 - k_{sl}h \\ 0 & F\lambda^2 + m\omega^2 & -F\lambda \\ -J\lambda^2 - k_{sl}h - J_1\omega^2 & F\lambda & I\lambda^2 - k_{sl}h^2 + I_1\omega^2 - F \end{vmatrix} U_1 = 0 \tag{43}$$

where, $|\ |$ represents the determinant of a matrix.

The solutions of vibration equations can be obtained by using the following expressions

$$\xi_1 = \sum_{i=1}^{6} a_i \beta_{1i} \exp(\lambda_i x) \tag{44}$$

$$w_1 = \sum_{i=1}^{6} a_i \beta_{2i} \exp(\lambda_i x) \tag{45}$$

$$\theta_1 = \sum_{i=1}^{6} a_i \beta_{3i} \exp(\lambda_i x) \tag{46}$$

$$\beta_i = \{\beta_{1i}, \beta_{2i}, 1\}^T \quad i = 1, 2, \cdots, 6 \tag{47}$$

$$\beta_{1i} = \frac{J\lambda^2 + J_1\omega^2 + k_{sl}h}{D\lambda^2 - k_{sl} + D_1\omega^2} \tag{48}$$

$$\beta_{2i} = \frac{F\lambda}{F\lambda^2 + m\omega^2} \tag{49}$$

where, $\{a_1, a_2, \ldots, a_6\}^T$ is the integration constant vector, λ_i is the characteristic root of the Eq. (43).

3.5 Solution for the natural vibration frequency

From Eqs. (33)-(35), the common boundary conditions of SCCTB can be obtained as:

(1) Natural boundary condition at simply supported end are

$$\xi'|_{x=0,L} = w|_{x=0,L} = \theta'|_{x=0,L} = 0 \tag{50}$$

(2) Natural boundary condition at fixed end are

$$\xi|_{x=0,L} = w|_{x=0,L} = \theta|_{x=0,L} = 0 \tag{51}$$

From Eqs. (50) and (51), it is clear that there are three natural boundary conditions at either end of the SCCTB. Substituting Eqs. (44)-(46) into the boundary conditions, six equations can be obtained. So the characteristic matrix equation of SCCTB with respect to the integration constant a_i can be expressed as

$$[B(\omega)]\{a_1, a_2, ..., a_6\}^T = 0 \tag{52}$$

Only the following is required to obtain the untrivial solution of the integration constant vector

$$|B(\omega)| = 0 \tag{53}$$

By using the MATLAB, a numerical calculation program is developed for solving the characteristic equation determinant, so that the natural vibration frequencies of SCCTB ω_i (i=1,2,…..) can be obtained.

3.6 Degeneration of vibration equations

In order to study the effect of shear deformation on natural vibration properties of SCCTB, in this paper, the degeneration is conducted on vibration equations and boundary conditions. It can help to obtain the vibration equations and boundary conditions without taking the influence of shear deformation

$$D\xi'' - k_{sl}(\xi + hw') - Jw''' + J_1\ddot{w}' - D_1\ddot{\xi} = 0 \tag{54}$$

$$Iw''' - J\xi'' - k_{sl}(\xi + hw')h + J_1\ddot{\xi} - m\ddot{w} - I_1\ddot{w}' = 0 \tag{55}$$

$$(D\xi' - Jw'')\delta\xi|_0^L = 0 \tag{56}$$

$$(Iw''' - J\xi'' - k_{sl}\zeta h + J_1\ddot{\xi} - I_1\ddot{w}')\,\delta w|_0^L = 0 \tag{57}$$

$$(Iw'' - J\xi')\delta w'|_0^L = 0 \tag{58}$$

The method of solving natural vibration frequency of SCCTB without considering the effect of shear deformation follows the similar procedure as mentioned above.

4. Computational examples

By taking into account two groups of SCCTBs with different spans as examples, where each group of SCCTBs contains five degrees of shear connections. The natural vibration frequencies of SCCTB were calculated by employing the analytical method and ANSYS finite element method. The mechanical and geometric parameters of SCCTBs are as follows: ρ_s=7900 kg·m^{-3}, μ_s=0.30, μ_c=0.20, ρ_c=2400 kg·m^{-3}, t_1=0.14 m, t_2=0.14 m, b_1=0.40 m, b_2=0.25 m, b_3=0.20 m, b_4=0.25 m, b_5=0.470 m, b_6=0.40 m, b_7=0.80 m, b_8=0.84 m, H_3=0.04 m, H_4=0.04 m, H_5=0.043 m, H_6=0.022 m, H_7=H_8=0.022 m, h_3=h_4=0.034 m, h_5=0.037 m, h_6=h_7=h_8=0.017 m, T_3=T_4=0.04 m, T_5=0.043 m, T_6=T_4=T_8=0.022 m, t_3=t_4=0.034 m, t_5=0.037 m, t_6=0.017 m, t_7=t_8=0.017 m, E_s=2.0×10^{11} N·m^{-2}, E_c=4.5×10^{10} N·m^{-2}, G_s=7.69×10^{10} N·m^{-2}, The span of SCCTB in Group 1 is L_1=10 m while in Group 2 is L_2=20 m. In order to verify the practicability of the above theoretical model, ANSYS finite element method was used for the simulation analysis. SOLID65 element was used to simulate the concrete slab. The SOLID65 element can simulate the nonlinear property of concrete. The element behaves as a linear elastic material until the stress reaches the tension or compression strength. After cracking, the tension stress of the concrete element is set to zero in the direction normal to the crack plane. The shear transfer coefficient β_t for open cracks and β_c for closed cracks determines the amount of shear transferred across the cracks. The value of the shear transfer coefficient ranges from 0.0 to 1.0, with 0.0 representing no shear transfer at a crack section and 1.0 representing full shear transfer. SHELL43 element was employed to simulate the chords. In order to ensure adequate studs between the chords and concrete slabs, the SHELL43 elements were subdivided into the same meshes as the concrete slabs. LINK8 element was used to simulate the web members, lower horizontal connections and oblique bracings. The LINK8 element is a spar which may be used in a variety of engineering applications. Depending upon the application, the element may be thought of as a truss element, a cable element, a link element, a spring element, etc. The three-dimensional spar element is a uniaxial tension-compression element with three degrees of freedom at each node. As in a pin-jointed structure, no bending of the element is considered. The element is defined by two nodes, the cross-sectional area, an initial strain, and the material properties. Therefore, based on small deformation assumption, the LINK8 element can be employed to simulate the oblique web member, vertical web member, lower horizontal connection member and oblique bracing member. The COMBIN14 element was used to simulate the stud

Table 1 Comparison of calculation results of natural vibration frequency of SCCTB with a span of 10 m

Degree of shear connection	Computing methods	Natural vibration frequency (Hz)					
		1st	2nd	3rd	4th	5th	6th
0.45	General composite truss beam theory	9.39	24.82	47.89	78.61	116.64	162.16
	Method considering influence of shear deformation	8.91	22.91	42.17	65.56	92.14	120.94
	ANSYS finite element method	9.07	22.80	41.74	65.34	93.49	126.15
	Effect of shear deformation (%)	5.35	8.33	13.58	19.90	26.59	34.08
	Calculation error (%)	-1.78	0.50	1.03	0.33	-1.45	-4.12
0.8	General composite truss beam theory	9.71	25.46	48.70	79.41	117.60	163.11
	Method considering influence of shear deformation	9.23	23.39	42.81	66.20	92.62	121.42
	ANSYS finite element method	9.33	23.14	42.09	65.66	93.78	126.41
	Effect of shear deformation (%)	5.17	8.84	13.75	19.95	26.97	34.34
	Calculation error (%)	-1.12	1.11	1.71	0.82	-1.24	-3.95
1.0	General composite truss beam theory	9.87	25.78	49.17	79.89	118.08	163.75
	Method considering influence of shear deformation	9.39	23.71	43.12	66.36	92.93	121.58
	ANSYS finite element method	9.45	23.30	42.27	65.83	93.94	126.55
	Effect of shear deformation (%)	5.08	8.72	14.02	20.38	27.05	34.68
	Calculation error (%)	-0.72	1.75	2.02	0.80	-1.07	-3.93
1.5	General composite truss beam theory	10.19	26.42	50.13	81.00	119.35	165.02
	Method considering influence of shear deformation	9.71	24.19	43.60	67.00	93.25	121.74
	ANSYS finite element method	9.70	23.67	42.68	66.23	94.30	126.89
	Effect of shear deformation (%)	5.11	8.73	14.45	20.39	27.49	35.04
	Calculation error (%)	0.06	2.22	2.16	1.15	-1.12	-4.06
2.0	General composite truss beam theory	10.50	27.05	50.92	82.11	120.47	166.30
	Method considering influence of shear deformation	10.03	24.67	44.24	67.63	93.89	122.38
	ANSYS finite element method	9.89	23.96	43.04	66.59	94.64	127.20
	Effect of shear deformation (%)	4.76	9.68	15.11	21.41	28.08	35.54
	Calculation error (%)	1.41	2.94	2.79	1.56	-0.63	-3.54
Average value of calculation error (%)		-0.43	1.71	2.02	0.98	-1.03	-3.84
Effect of interface slip (%)		8.95	5.09	3.12	1.91	1.23	0.83

connectors, a group of which was used as the equivalent of one single stud to avoid the calculation of non-convergence caused by the stress concentration of studs. The COMBIN14 element is a spring-damper element, which has longitudinal or torsional capability in 1D, 2D, or 3D applications. The longitudinal spring-damper option is a uniaxial tension-compression element with up to three degrees of freedom at each node. No bending or torsion is considered. The torsional spring-damper option is a purely rotational element with three degrees of freedom at each node. No bending or axial loads are considered. The elastic modulus of the spring element was calculated by using Eq. (17). The vertical interactions at the interface between the concrete slab and steel beam were achieved by coupling the free degrees in the vertical direction of the nodes at the same position, i.e., ignoring the vertical separation between concrete slab and steel truss beam. The simulation results are compared against the theoretical results, as shown in Tables 1-2.

It can be seen from Tables 1-2 and Figs. 3-4 that: the computational theory proposed in this paper and ANSYS finite element method in the calculation of the first 6-order natural vibration frequencies of the two groups of SCCTB are in good agreement with each other. Moreover, the error does not exceed 4.2%, which proves the accuracy of the theory method applied in this paper.

The interface slip effect on the SCCTB's natural vibration frequencies decreases with the increase in the

Table 2 Comparison of calculation results of natural vibration frequency of SCCTB with a span of 12 m

Degree of shear connection	Computing methods	Natural vibration frequency (Hz)					
		1st	2nd	3rd	4th	5th	6th
0.45	General composite truss beam theory	6.52	17.34	33.41	54.74	81.32	112.98
	Method considering influence of shear deformation	6.36	16.39	30.55	47.89	68.11	90.39
	ANSYS finite element method	6.50	16.43	30.19	47.31	67.62	91.07
	Effect of shear deformation (%)	2.50	5.82	9.38	14.28	19.40	25.00
	Calculation error (%)	-2.11	-0.27	1.21	1.25	0.71	-0.75
0.8	General composite truss beam theory	6.84	17.82	34.05	55.53	81.95	113.78
	Method considering influence of shear deformation	6.68	16.86	31.03	48.37	68.58	90.86
	ANSYS finite element method	6.72	16.74	30.52	47.62	67.91	91.32
	Effect of shear deformation (%)	2.38	5.66	9.74	14.80	19.49	25.22
	Calculation error (%)	-0.56	0.79	1.68	1.60	1.00	-0.50
1.0	General composite truss beam theory	7.00	18.14	34.37	55.86	82.43	114.26
	Method considering influence of shear deformation	6.68	17.03	31.19	48.69	68.91	91.18
	ANSYS finite element method	6.82	16.88	30.69	47.78	68.06	91.46
	Effect of shear deformation (%)	4.76	6.54	10.20	14.70	19.63	25.31
	Calculation error (%)	-2.01	0.85	1.63	1.91	1.25	-0.30
1.5	General composite truss beam theory	7.16	18.62	35.17	56.81	83.39	115.37
	Method considering influence of shear deformation	7.00	17.50	31.82	49.33	69.54	91.66
	ANSYS finite element method	7.02	17.20	31.07	48.16	68.41	91.79
	Effect of shear deformation (%)	2.27	6.36	10.50	15.16	19.91	25.87
	Calculation error (%)	-0.23	1.77	2.45	2.43	1.64	-0.13
2.0	General composite truss beam theory	7.48	19.09	35.80	57.60	84.34	116.33
	Method considering influence of shear deformation	7.16	17.82	32.30	49.81	70.02	92.29
	ANSYS finite element method	7.16	17.46	31.39	48.50	68.74	92.09
	Effect of shear deformation (%)	4.44	7.14	10.84	15.65	20.45	26.03
	Calculation error (%)	0.08	2.09	2.91	2.71	1.86	0.22
Average value of calculation error (%)		-0.99	1.04	1.87	1.98	1.30	-0.29
Effect of interface slip (%)		10.15	6.23	3.97	2.51	1.65	1.12

natural vibration frequency. On the other hand, the SCCTB's shear deformation effect increases with the increase in natural vibration frequency. The analysis indicates that the low-order vibration mode curve of SCCTB is mainly composed of cross-section rotation deformation, while the shear deformation only plays a small part in the low-order vibration mode curve.

The interface slip effect on SCCTB's low-order natural vibration frequencies is greater than 10%. The shear deformation effect on SCCTB's low-order natural vibration frequencies is found to be small, while that of the high-order natural vibration frequencies is found more than 35%. The overall analysis indicates that the influence of interface slip and shear deformation on natural vibration frequencies of SCCTB cannot be neglected.

5. Conclusions

Based on the concept of transformed section and displacement superposition, the calculation method of SCCTB's natural vibration frequency is developed. The derivation of the calculation method in this paper is theoretically appropriate. Through the theoretical calculation and finite element numerical simulations of 10 SCCTBs with different degrees of shear connection and effective spans as examples, the following conclusions are obtained:

- Comprehensively, by considering the influence of shear deformation, interface slip and moment of inertia, the theoretically calculated results of SCCTB's natural vibration frequencies are found to be in good agreement

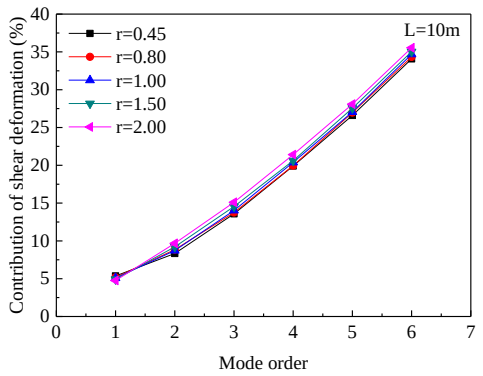

(a) L=10 m

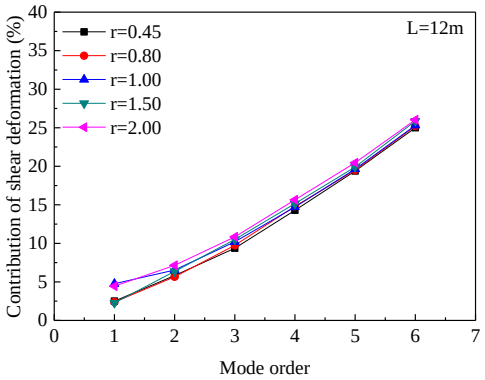

(b) L=12 m

Fig. 3 Relationship between contribution of shear deformation and the mode orders of flexural natural vibration

with the finite element numerical results, which proves the correctness of the developed method.

• The shear deformation effect of SCCTB's low-order natural vibration frequencies is small.

• The SCCTB's shear deformation effect increases with the increase in natural vibration frequency. The calculation result of SCCTB's natural vibration frequency would be much larger than the actual result, when the shear deformation is not taken into account.

• The interface slip effect of SCCTB's natural vibration frequencies decreases with the increase in natural vibration frequency, and the interface slip effect on the low-order natural vibration frequencies is found to be more than 10%. Therefore, the effect of interface slip on the natural vibration frequencies of SCCTB cannot be ignored.

• SCCTB's low-order vibration mode curves are mainly composed of cross-section rotation deformations, while shear deformation plays a small part in the low-order vibration mode curves.

Acknowledgments

The research described in this paper was financially supported by the National Natural Science Foundation of China (51408449, 51378502, 51778630), the Innovation-driven Plan in Central South University under grant (2015CX006).

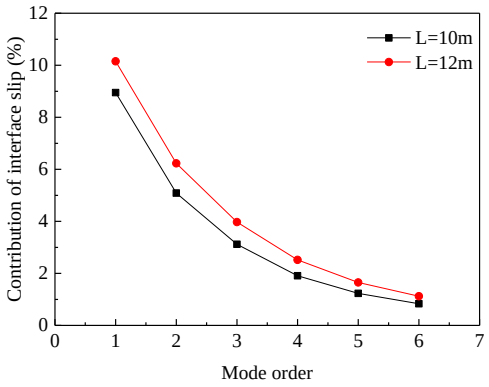

Fig. 4 Relationship between the interface slip effect and the mode orders of flexural natural vibration

References

Aiello, M.A. (2008), "Analisi sperimentale della connessione acciaio-calcestruzzo nelle travi reticolari miste (Experimental analysis of steel–concrete connection in hybrid truss beams)", *Proceeding of 7th Italian Workshop on Composite Structures*.

Bouchair, A., Bujnak, J. and Duratna, P. (2012), "Connection in steel-concrete composite truss", *Procedia Eng.*, **40**, 96-101.

Bujnak, J. and Bouchair, A. (2014), "Theoretical and experimental research on steel concrete composite truss", *IABSE Symposium Report International Association for Bridge and Structural Engineering*, **102**(19), 1749-1756.

Campione, G., Colajanni, P. and Monaco, A. (2016), "Analytical evaluation of steel-concrete composite trussed beam shear capacity", *Mater. Struct.*, **49**(8), 3159-3176.

Chan, S.L. and Fong, M. (2011a), "Experimental and analytical investigations of steel and composite trusses", *Conference paper Advanced Steel Construction*, **26**, 1-17.

Colajanni, P., La Mendola, L. and Monaco, A. (2014), "Stress transfer mechanism investigation in hybrid steel trussed-concrete beams by push-out tests", *J. Constr. Steel Res.*, **95**, 56-70.

Colajanni, P., La Mendola, L., Latour, M., Monaco, A. and Rizzano, G. (2015a), "FEM analysis of push-out test response of Hybrid Steel Trussed Concrete Beams (HSTCBs)", *J. Constr. Steel Res.*, **111**, 88-102.

Colajanni, P., La Mendola, L. and Monaco, A. (2015b), "Stiffness and strength of composite truss beam to RC column connection in MRFs", *J. Constr. Steel. Res.*, **113**, 86-100.

Colajanni, P., La Mendola, L., Latour, M., Monaco, A. and Rizzano, G. (2017), "Analytical prediction of the shear connection capacity in composite steel-concrete trussed beams", *Mater. Struct.*, **50**(1), 48.

Ding, F., Liu, J., Liu, X., Guo, F. and Jiang, L. (2016), "Flexural stiffness of steel-concrete composite beam under positive moment", *Steel Compos. Struct.*, **20**(6), 1369-1389.

Duratna, P., Bujnak, J. and Bouchair, A. (2013), "Behavior of steel-concrete composite trusses", *Pollack Periodica*, **8**(2), 23-28.

Fong, M., Chan, S.L. and Uy, B. (2011b), "Advanced design for trusses of steel and concrete-filled tubular sections", *Eng. Struct.*, **33**(12), 3162-3171.

Giltner, B. and Kassimali, A. (2000), "Equivalent beam method for trusses", *Pract. Period. Struct. Des. Constr.*, **5**(2), 70-77.

Han, Q., Yuan, Z., Ying, M. and Liu, X. (2005), "Numerical analysis and experimental study of prestressed diagonal-on-square composite space truss", *Adv. Struct. Eng.*, **8**(4), 397-410.

Han, Q.H. (2004), "Analysis of natural vibration characteristics and testing on construction site of pre-stressed composite space

truss", *Earthq. Eng. Eng. Vib.*, **24**(2), 118-124.
Liu, J., Ding, F., Liu, X. and Yu, Z. (2016), "Study on flexural capacity of simply supported steel-concrete composite beam", *Steel Compos. Struct.*, **21**(4), 829-847.
Machacek, J. and Cudejko, M. (2009), "Longitudinal shear in composite steel and concrete trusses", *Eng. Struct.*, **31**(6), 1313-1320.
Machacek, J. and Cudejko, M. (2010), "Shear connection in steel and concrete composite trusses", *SDSS'Rio 2010 Stability and Ductility of Steel Structures*, 8-10.
Machacek, J. and Cudejko, M. (2011), "Composite steel and concrete bridge trusses", *Eng. Struct.*, **33**(12), 3136-3142.
Morassi, A., Nakamura, G., Shirota, K. and Sini, M. (2007), "A variational approach for an inverse dynamical problem for composite beams", *Eur. J. Appl. Math.*, **18**(1), 21-55.
Nie, J., Cai, C.S. and Wang, T. (2005), "Stiffness and capacity of steel-concrete composite beams with profiled sheeting", *Eng. Struct.*, **27**(7), 1074-1085.
Nie, J., Fan, J. and Cai, C.S. (2004), "Stiffness and deflection of steel-concrete composite beams under negative bending", *J. Struct. Eng.*, **130**(11), 1842-1851.
Nie, J.G., Cai, C.S., Zhou, T.R. and Li, Y. (2007), "Experimental and analytical study of prestressed steel-concrete composite beams considering slip effect", *J. Struct. Eng.*, **133**(4), 530-540.
Siekierski, W. (2016a), "An analytical method to estimate the natural bending frequency of the spans of railway through truss bridges with steel and concrete composite decks", *Proceedings of the Institution of Mechanical Engineers, Part F: Journal of Rail and Rapid Transit*, **230**(8), 1908-1918.
Siekierski, W. (2016b), "Analysis of concrete shrinkage along truss bridge with steel-concrete composite deck", *Steel Compos. Struct.*, **20**(6), 1237-1257.
Zhou, L., Yu, Z. and He, G. (2013), "A new 3-D element formulation on displacement of steel-concrete composite box beam", *J. Cent. South Univ.*, **20**(5), 1354-1360.
Zhou, W., Jiang, L., Huang, Z. and Li, S. (2016), "Flexural natural vibration characteristics of composite beam considering shear deformation and interface slip", *Steel Compos. Struct.*, **20**(5), 1023-1042.
Zhou, W., Jiang, L., Yu, Z. and Huang, Z. (2013), "Analysis of free vibration characteristics of steel-concrete composite continuous box girder considering shear lag and slip", *J. Cent. South Univ.*, **20**(9), 2570-2577.
Zhou, W., Li, S.J., Jiang, L. and Qin, S. (2015), "Vibration analysis of steel-concrete composite box beams considering shear lag and slip", *Math. Probl. Eng.*, **2015**, 1-8.
Zhou, W.B., Jiang, L.Z., Liu, Z.J. and Liu, X.J. (2012), "Closed-form solution to thin-walled box girders considering effects of shear deformation and shear lag", *J. Cent. South Univ.*, **19**(9), 2650-2655.

CC